Computational Materials Science 82 (2014) 314–319

Contents lists available at ScienceDirect

Computational Materials Science

journal homepage: www.elsevier.com/locate/commatsci

Numerical analysis of the indentation size effect using a strain gradient crystal plasticity model

D. González, J. Alkorta, J.M. Martínez-Esnaola *, J. Gil Sevillano

CEIT and TECNUN (University of Navarra), P. Manuel Lardizabal 15, 20018 San Sebastián, Spain

ARTICLE INFO

Article history:
Received 18 July 2013
Received in revised form 24 September 2013
Accepted 1 October 2013
Available online 30 October 2013

Keywords:
Indentation size effect (ISE)
Crystal plasticity
Strain gradient
Geometrically necessary dislocations
Hardness measurement
Finite element method

ABSTRACT

This work presents a finite element analysis of the indentation size effect (ISE) experimentally observed in tests performed at submicron scale. A 3D model of a conical rigid surface indenting on a Nb single crystal at different depths has been developed. The bcc Nb material has been characterized within a finite-strain framework through a crystal plasticity model incorporating strain-gradient hardening. The hardness evolution for different material orientations and for different initial dislocation densities has been studied. The numerical results are compared with predictions of existing analytical models and with experimental results.

1. Introduction

From an experimental point of view, the indentation size effect (ISE) is a well-known phenomenon that becomes apparent at submicron scale with a decrease in the hardness measure as the indentation depth increases. Numerous works have reported the ISE experimentally, with different types of materials and arrangements [1–6].

The analytical model of Nix and Gao [5] suggests a linear relationship between the square of the hardness and the inverse of the penetration depth. Many studies have confirmed this linearity above a certain depth; however, more detailed inspections at extremely low indentation depths show a deviation from this linearity [7–10]. In this work, we try to cast some light on this problem. The objective is to study the ISE from a numerical point of view with the aid of a finite element (FE) model of an indentation experiment. For this purpose, a 3D model consisting of a conical rigid surface with a round tip indenting on a single crystal of Nb has been constructed. The bcc material has been simulated by means of a crystal plasticity model, implemented within a finite-strain framework. Of capital importance, the size effect phenomenon present in the experiments has been captured in the simulation work incorporating a strain-gradient formulation in the constitutive equations of the material model. The general-purpose FE program ABAQUS has been used in this analysis, complemented via FORTRAN user subroutines.

Among the pioneering analysis on strain-gradient plasticity, of special relevance is the numerical work of Fleck and Hutchinson [11,12]. Their plastic models capture the strain-gradient effects using a set of the so-called 'material lengths' within a coupled-stress general framework. These phenomenological length measures are necessary in their formulation to calculate an equivalent local strain, acting as scaling factors of a close-related measure of the strain-gradient value, obtained with the second derivatives of the displacement field. A dependence of the material hardening on other magnitudes apart from the strain is therefore established, in contrast with the conventional plasticity theories.

As previously mentioned, the material model defined here also considers a strain gradient measure, though a different approach is used to estimate its influence in the material hardening equations. The constitutive equations descend to the crystallographic slip nature of plastic deformation, and, under this crystallographic framework, a local density of geometrically necessary dislocations (GND) is defined. The GND concept appears in this model closely linked to the strain gradient measure, as the works of Nye [13] and Fleck et al. [14] show. In order to prove and explain the ISE effect with this material model, a series of different indentation depths, ranging from 0.01 μm to 66 μm, have been performed on the Nb material model described.

The numerical results obtained have been compared with those predicted by the analytical models of Nix and Gao [5] – calculated for a perfectly sharp tip – and Alkorta et al. [6] – that improves the previous one by adding a rounded tip to the conical indenter and

* Corresponding author. Tel.: +34 943 212800.
E-mail addresses: dgonzalez@ceit.es (D. González), jalkorta@ceit.es (J. Alkorta), jmesnaola@ceit.es (J.M. Martínez-Esnaola), jgil@ceit.es (J. Gil Sevillano).

0927-0256/$ - see front matter © 2013 Elsevier B.V. All rights reserved.
http://dx.doi.org/10.1016/j.commatsci.2013.10.004

by considering the dependence of dislocation strengthening on the current dislocation density. Both models work with average statistically stored dislocation (SSD) and GND densities estimated in a semispherical volume underneath the indenter tip, establishing a trend for the hardness value evolution with the indenter depth and explaining the ISE. The numerical results of this paper have also been confronted with experimental measurements obtained on individual grains of polycrystalline Nb [6].

2. Model

The indentation process has been simulated by means of an FE model, with a rigid conical surface – with an angle of 19.7° – indenting on a semispherical volume of elasto-plastic material (see Fig. 1). The radius of the indenter tip is 0.01 μm and its contact with the Nb material has been defined as frictionless, using a stiff exponential law in normal direction.

Three different crystallographic orientations have been studied for the Nb material, i.e., ⟨001⟩, ⟨011⟩ and ⟨111⟩, using the ⟨001⟩ orientation as the reference one. For this case, a portion of 45° of the semispherical material volume has been modelled (as shown in Fig. 1), considering all the symmetries present in the problem – geometric, crystallographic and elastic.

In order to study the hardness evolution with the indentation depth, eight different depth values have been considered, ranging from 0.01 μm to 66 μm, as Table 1 summarizes. A detailed curve of the hardness as a function of the indentation depth has been obtained for all the cases, with a different average of the depth increments for each case within the incremental solution method employed. Given the wide range of the analysed indentation depths, an appropriate element size has to be set for each case. For that reason, a unique mesh has been built, scaling its dimensions with the corresponding indentation depth of each case. Thus, eight different models have been studied, working that way with an adequate mesh size for the depth of study in each model. Table 1 also collects the element size underneath the indenter for each case.

Apart from the scaling of the mesh dimensions with the indentation depth, all the other aspects of the simulation are the same for the eight cases. The boundary conditions are illustrated in Fig. 1, with symmetry conditions in both lateral planes of the volume, and the nodes of the spherical bound with null displacements imposed. The mesh is constituted by 20,000 first-order eight-noded isoparametric elements (C3D8 in ABAQUS nomenclature).

The driving force of the simulations is the displacement of the indenter, imposed as a boundary condition. An exponential time dependence of this displacement, h, has been defined,

$$h = ke^{\dot{\varepsilon}_0 t} - k \tag{1}$$

so as to obtain an almost constant strain rate ($\dot{h}/h \approx \dot{\varepsilon}_0 = 0.12\ s^{-1}$) for all the simulations of the analysis from a certain time instant. The constant k has been defined for each case in order to accomplish with the specific indentation depth (k values are collected in Table 1). The time of indentation chosen for all the simulations is 100 s.

The material constitutive model has been implemented at integration point level through a user subroutine (UMATEL in ABAQUS nomenclature), complemented with other home-made subroutines. A finite-strain analysis has been developed based on the Green–Lagrange strain tensor, $\mathbf{E}$, and its corresponding work conjugate stress tensor, i.e., the second Piola–Kirchhoff stress tensor, $\mathbf{T}$. The usual multiplicative decomposition of the deformation gradient $\mathbf{F}$ into its elastic (plus possible rigid body motions) and plastic parts, respectively, $\mathbf{F}^e$ and $\mathbf{F}^p$, has been used,

$$\mathbf{F} = \mathbf{F}^e \cdot \mathbf{F}^p. \tag{2}$$

In this formulation, the crystal kinematics assumes a *virtual* intermediate configuration, between the reference initial position of the solid and the deformed configuration, where only plastic strain has taken place, with the orientation of the crystal lattice remaining unchanged [15–17].

The relation of the Green–Lagrange strain, defined with the elastic deformation gradient, with the Piola–Kirchhoff stress through an elastic orthotropic fourth-order tensor Π has been chosen as the governing equation of the algorithm,

$$\mathbf{T} = \Pi : \mathbf{E}^e \tag{3}$$

with $\mathbf{E}^e = \frac{1}{2}(\mathbf{F}^{eT}\mathbf{F}^e - \mathbf{I})$. The crystal plasticity theory defines the plastic velocity gradient in the intermediate configuration, $\mathbf{L}^p$, by means of the plastic slip rates in each slip system α, $\dot{\gamma}^\alpha$, as

$$\mathbf{L}^p = \sum_\alpha \dot{\gamma}^\alpha \mathbf{m}^\alpha \otimes \mathbf{n}^\alpha = \sum_\alpha \dot{\gamma}^\alpha \mathbf{S}^\alpha \tag{4}$$

where $\mathbf{n}^\alpha$ and $\mathbf{m}^\alpha$ are orthonormal unit vectors that define the slip plane normal and the slip direction, respectively, of the slip system α in the reference and intermediate configurations.

The plastic slip systems considered in the modelled bcc material are those corresponding to the families {110}⟨111⟩ and {112}⟨111⟩ (12 systems in each family), which are assumed to evolve following a uniform hardening law, see below. Within the

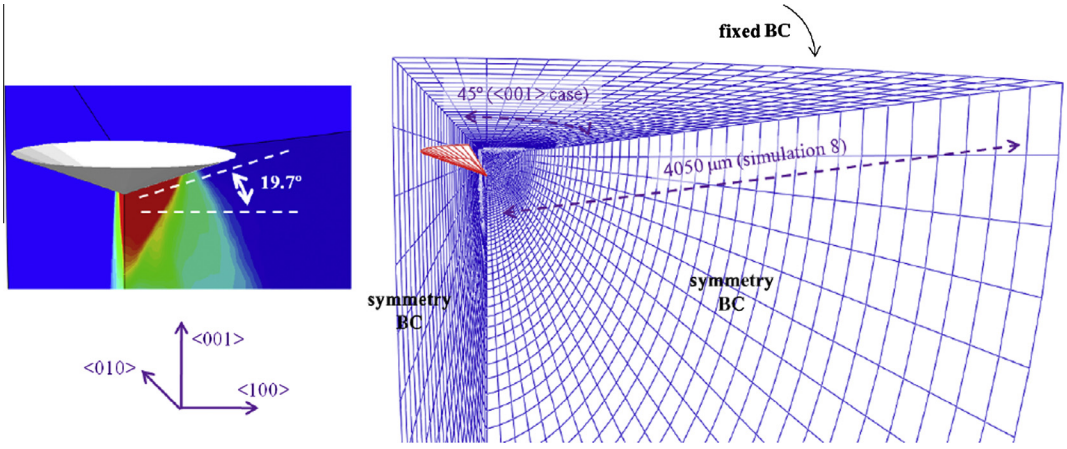

Fig. 1. Boundary conditions of the indentation model. The radius of the semispherical volume in the models is large enough to prevent any border effect due to the constrained boundary conditions imposed at the external semispherical bound.